

# Gate-All-Around Single-Crystal-Like Poly-Si Nanowire TFTs With a Steep-Subthreshold Slope

Tung-Yu Liu, Shen-Chuan Lo, and Jeng-Tzong Sheu

**Abstract**—We investigate the characteristics of single-crystal-like (SCL) poly-Si nanowire (SCL poly-Si NW) thin-film-transistors with gate-all-around (GAA) structures. The GAA SCL poly-Si NWs are prepared by a modified sidewall spacer process utilizing an amorphous silicon ( $\alpha$ -Si) mesa structure. The combination of the high surface-to-volume ratio of the NW and a nominal gate length of  $0.25\ \mu\text{m}$  lead to clear improvement in electrical performance, including a steep subthreshold swing ( $90 \pm 15\ \text{mV/dec}$ ), a virtual absence of drain-induced barrier lowering ( $21 \pm 13\ \text{mV/V}$ ), and a very high ON/OFF current ratio  $\sim 7 \times 10^7$  ( $V_D = 1\ \text{V}$ ,  $V_G = 3\ \text{V}$ ).

**Index Terms**—Gate-all-around (GAA), nanowire (NW), single-crystal-like (SCL), thin film transistor (TFT).

## I. INTRODUCTION

DEUE TO the simplicity in device preparation and excellent performance in electrical properties, polycrystalline silicon thin-film transistors (Poly-Si TFTs) have been studied and applied in many applications, such as active matrix liquid crystal displays [1] and memory devices [2]. Recently, poly-Si TFTs utilizing nanowire (NW) channel with multiple-gate structures have been demonstrated to meet demands in both TFT performance and suppression of short channel effects encountered during scale-down [3]–[5]. Although gate controllability was enhanced through multiple-gate structures, defects at grain boundaries and dangling bonds in the poly-Si NW channel undermine the carrier mobility and the device switching speed [6]. Different techniques such as solid-phase crystallization (SPC) [7], metal-induced-lateral crystallization [8], and excimer laser annealing [9] have been proposed to increase the grain size so that trap-state density can be reduced. Plasma treatment has also been demonstrated to reduce the defect density [5], [10]. In addition, reduction of defect density and improvement of gate controllability via scale-down of the poly-Si NW channel have been reported. Some studies have even demonstrated the scale-down of the poly-Si NW without using advanced lithographic tools and have obtained excellent device characteristics [11]–[14]. Poly-Si NW TFTs with small gate length ( $< 0.1\ \mu\text{m}$ ) and very thin dielectrics have also been proposed to improved transfer characteristics

Manuscript received October 4, 2012; accepted February 12, 2013. Date of publication March 7, 2013; date of current version March 20, 2013. The review of this letter was arranged by Editor K. Uchida.

T.-Y. Liu and J.-T. Sheu are with the Department of Materials Science and Engineering, Institute of Nanotechnology, National Chiao Tung University, Hsinchu 30050, Taiwan (e-mail: jtshieu@faculty.nctu.edu.tw).

S.-C. Lo is with the Material and Chemical Research Laboratories, Industrial Technology Research Institute, Hsinchu 31040, Taiwan.

Color versions of one or more of the figures in this letter are available online at <http://ieeexplore.ieee.org>.

Digital Object Identifier 10.1109/LED.2013.2247737

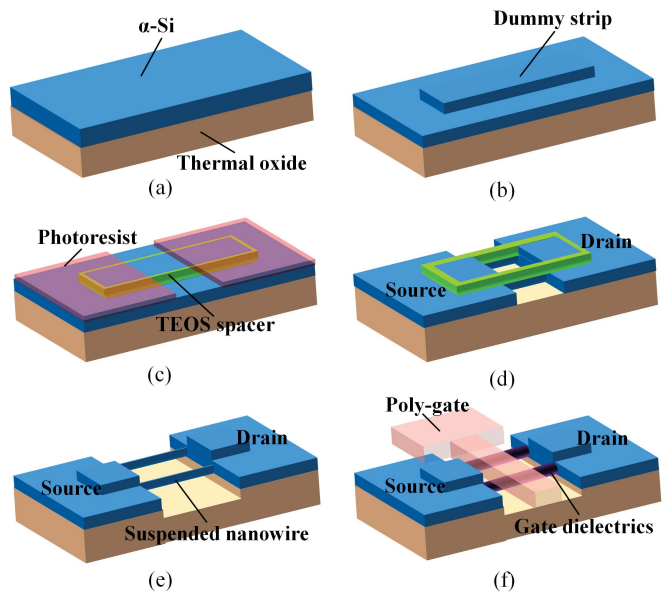


Fig. 1. (a)–(f) Key process flow of device fabrication using the simplified sidewall spacer technique.

[15], [16]. However, short-channel effects (SCEs) like large leakage current and drain-induced barrier lowering (DIBL) have emerged as problems. Therefore, poly-Si TFT with the GAA structure still suffers from intrinsic defects in the poly-Si channel. In this letter, we present a novel modified sidewall spacer process to prepare poly-Si NW TFTs with a gate-all-around (GAA) structure. The nanowire channel exhibits SCL structure after SPC process. Without any trap-reduced plasma treatment, the GAA SCL poly-Si NW TFTs possessing channels of high surface-to-volume ratio and a  $0.25\text{-}\mu\text{m}$  gate length exhibited superior channel controllability and the ability to suppress SCEs.

## II. DEVICE FABRICATION

The GAA SCL poly-Si NW TFTs were fabricated by a simplified top-down sidewall spacer technique, with the key process flow shown in Fig. 1. Wafers with 500-nm thick thermal oxide were grown as the starting substrate layer, and a 70-nm thick amorphous silicon ( $\alpha$ -Si) layer was deposited using low pressure chemical vapor deposition (LPCVD) at  $550\ ^\circ\text{C}$  [Fig. 1(a)]. Next, the  $\alpha$ -Si layer was patterned into a mesa structure through optical lithography, which was followed by reactive ion etching (RIE). The  $\alpha$ -Si layer was transformed into two parts; the thicker part served as a

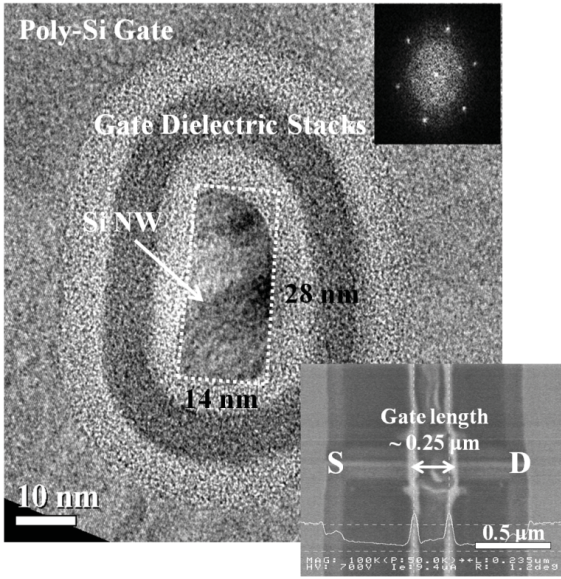


Fig. 2. Cross-section TEM image of a GAA SCL poly-Si NW TFT. The NW was surrounded by gate dielectric stacks ( $\text{ONO} = 5 \text{ nm}/8 \text{ nm}/8 \text{ nm}$ ) and a poly-Si gate. Upper inset: FFT patterns confirming the zone axis of the Si NWs is in the [110] direction. Lower inset: SEM image confirming the gate length of the GAA SCL poly-Si NW TFT is around  $0.25 \mu\text{m}$ .

dummy strip, and the thinner one served as device active layer [Fig. 1(b)]. A 60-nm thick tetraethylorthosilicate (TEOS) layer was deposited using LPCVD, and then etched through RIE, leaving TEOS spacers. Before NW formation, the source and drain (S/D) regions were defined through an I-line stepper [Fig. 1(c)]. Next, the  $\alpha$ -Si layer was etched through high-selective RIE, and the NWs were formed through TEOS hard masks [Fig. 1(d)]. After NWs formation, the TEOS hard masks were removed in 1:50 diluted HF solution. Next, the SPC was performed at  $600^\circ\text{C}$  for 24 h in nitrogen ambient to turn the  $\alpha$ -Si into polycrystalline silicon. Then the NWs were released from the bottom thermal oxide during the RCA cleaning [Fig. 1(e)]. The TEOS oxide/ nitride/ TEOS oxide ( $\text{O}/\text{N}/\text{O} = 5 \text{ nm}/8 \text{ nm}/8 \text{ nm}$ ) gate dielectric stacks and a 200-nm in situ  $\text{N}^+$ doped poly-Si film were placed surrounding NWs by using LPCVD conformal deposition. After the patterning of the poly-Si gate [Fig. 1(f)], the wafers were doped with phosphorus for the S/D at a dose of  $5 \times 10^{15} \text{ cm}^{-2}$  (10 keV) through self-aligned implantation to reduce the contact resistance and the series resistance of the S/D access regions. A 300-nm thick TEOS layer was deposited as the passivation layer using LPCVD. Then, samples were activated at  $600^\circ\text{C}$  for 8 h in nitrogen ambient. The contact holes were defined, and Al metallization was performed. Finally, the wafers were sintered at  $450^\circ\text{C}$  in a mixture of hydrogen (5%) and nitrogen (95%) ambient for 30 min. Despite the fact that the  $\text{O}/\text{N}/\text{O}$  gate stack undermines gate controllability, this poly-Si NW TFT device with surrounding ONO layers were prepared for potential memory applications.

### III. RESULTS AND DISCUSSION

Fig. 2 presents the high-resolution TEM channel cross-section image of a GAA SCL poly-Si NW TFT. The NW

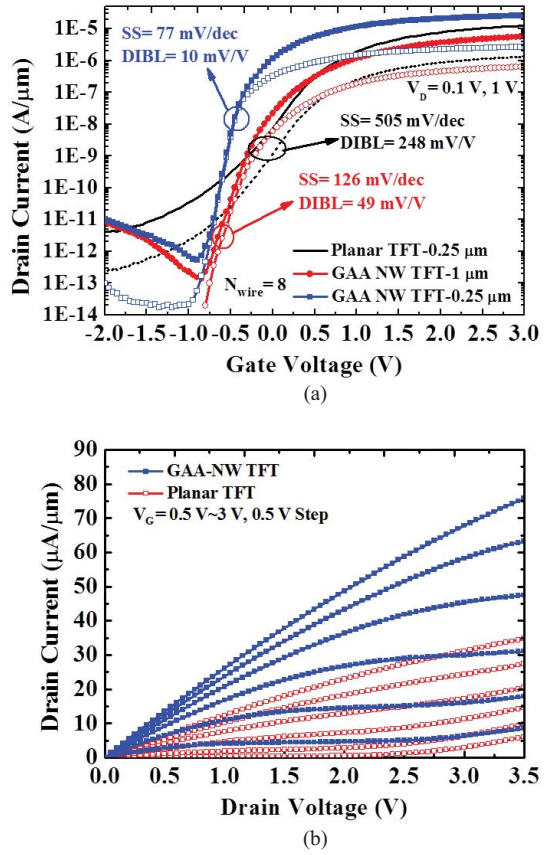


Fig. 3. (a) Transfer characteristics for a GAA SCL poly-Si NW TFT (gate lengths of  $0.25 \mu\text{m}$  and  $1 \mu\text{m}$ ) and conventional planar TFT. (b) Comparison of output characteristics between the GAA SCL poly-Si NW TFT and conventional planar TFT.

channel is surrounded by ONO stacks (TEOS/nitride/TEOS =  $5 \text{ nm}/8 \text{ nm}/8 \text{ nm}$ ) and a poly-Si gate with channel width  $\sim 14 \text{ nm}$  and thickness  $\sim 28 \text{ nm}$ . The upper inset is fast Fourier transform (FFT) patterns confirming that the zone axis of the Si NWs is the [110] direction. The FFT pattern also shows that the Si NWs are highly crystalline. The lower inset SEM image confirms that the gate length of GAA SCL poly-Si NW TFT is  $\sim 0.25 \mu\text{m}$ . In the process flow, the TEOS oxide was used as a sidewall hard mask instead of traditional silicon nitride hard mask. Without using the time-consuming wet etching process to remove silicon nitride and the additional dummy layer material, GAA SCL poly-Si NWs can be prepared efficiently with an improved device yield.

Fig. 3(a) presents a comparison of the normalized transfer characteristics ( $I_D$ - $V_G$  curve) between the GAA SCL poly-Si NW TFT and a planar TFT without any plasma-related treatment. The gate lengths of the TFTs were  $0.25 \mu\text{m}$ , and the effective width of the GAA SCL poly-Si NW and planar TFTs were  $0.672 \mu\text{m}$  ( $84 \text{ nm} \times 8$ ) and  $1.1 \mu\text{m}$ , respectively. The GAA SCL poly-Si NW TFT exhibits a threshold voltage of  $\sim -0.4 \text{ V}$  at  $I_D = (W_{\text{eff}}/L) \times 10^{-8} \text{ A}$  and  $V_D = 0.1 \text{ V}$ . An analysis of 24 TFTs showed that the GAA SCL poly-Si NW TFT exhibits a very small subthreshold swing ( $90 \pm 15 \text{ mV/dec}$ , extracted from  $I_D = 10^{-8} \text{ A}$  to  $I_D = 10^{-12} \text{ A}$  and  $V_D = 0.1 \text{ V}$ ), one which is superior to that of the planar

TABLE I  
CHARACTERISTICS OF RECENTLY REPORTED POLY-SI  
NW TFTS USING SPC TECHNIQUE

Source	This Letter	[5]	[14]	[15]	[16]
Gate structure	GAA	GAA	Double-gated	$\Omega$ -gate	$\Omega$ -gate
Gate length ( $\mu\text{m}$ )	0.25	2	1	0.1	0.09
Channel dimension ( $\text{nm}^2$ )	$14 \times 28$	$75 \times 38$	$18 \times 72$	$14 \times 17$	$20 \times 10$
NH <sub>3</sub> plasma treatment	W/O	1 h	3 h	W/O	W/O
EOT (nm)	18	20	20	1.7	10 (HfO <sub>2</sub> )
S.S. (mV/dec)	$90 \pm 15$	114	115	79	113
DIBL (mV/V)	$21 \pm 13$	13	60	78	251
I <sub>ON</sub> /I <sub>OFF</sub> ( $V_G; V_D$ )	$>10^7$ 3 V; 1 V	$>10^8$ 6 V; 3 V	$>10^7$ 6 V; 3 V	$>10^4$ 1 V; 1 V	$>10^7$ 6 V; 1 V

device ( $396 \pm 57$  mV/dec). Furthermore, the DIBL of the GAA SCL poly-Si NW and planar TFTs are  $21 \pm 13$  mV/V and  $237 \pm 97$  mV/V (extracted from  $\Delta V_{gs}/\Delta V_{ds}$  of  $V_D = 0.1$  and 1 V at  $I_D = 10^{-10}$  A), respectively. Furthermore, we suspect that large variations in both SS and DIBL could be further improved by increasing the grain size under the gate. The  $0.25\text{-}\mu\text{m}$  planar device exhibits SCEs, including a large SS and a clear DIBL due to inferior gate controllability. However, the  $0.25\text{-}\mu\text{m}$  GAA poly-Si NW TFT shows gate-induced leakage current (GIDL) in the OFF state as the result of stronger electric field between the gate and drain. The transfer characteristics of a  $1\text{-}\mu\text{m}$  GAA poly-Si NW TFT are also shown in Fig. 3(a). Despite the  $1\text{-}\mu\text{m}$  device exhibiting a lower leakage current, the  $0.25\text{-}\mu\text{m}$  device exhibits superior transfer characteristics owing to the short gate length and the reduction of grain boundaries under the gate area. We suspect that the gate length between  $0.1\text{ }\mu\text{m}$  and  $0.25\text{ }\mu\text{m}$  may be an appropriate length for further improvement of device characteristics. Fig. 3(b) presents a comparison of output characteristics between GAA SCL poly-Si NW and conventional planar TFTs. The proposed NW device exhibits a saturation current improvement of 223% at  $V_G = 3$  V and  $V_D = 3.5$  V (NW TFT  $\sim 76\text{ }\mu\text{A}/\mu\text{m}$  over the planar device  $\sim 34\text{ }\mu\text{A}/\mu\text{m}$ ). Table I shows a performance summary for the recently reported poly-Si NW TFTs using the SPC technique [5], [14]–[16]. Poly-Si NW TFTs with low SS and high ON/OFF current ratio were most usually subjected to NH<sub>3</sub> plasma treatment. In the absence of a lightly doped drain, devices with a gate length smaller than  $0.1\text{ }\mu\text{m}$  usually suffered from SCEs. However, this GAA SCL poly-Si NW TFT with a  $0.25\text{-}\mu\text{m}$  gate length and a very small NW channel ( $14 \times 28\text{ nm}^2$ ) exhibited single-crystal like electrical properties.

#### IV. CONCLUSION

We characterized GAA SCL poly-Si NW TFTs prepared by a novel modified side-wall spacer technique. Without the

need for plasma treatment, the GAA SCL poly-Si NW TFTs showed an excellent S.S. ( $90 \pm 15$  mV/dec), a very small DIBL ( $21 \pm 13$  mV/V), and a high ON/OFF current ratio  $\sim 7 \times 10^7$  at a relatively low voltage condition ( $V_G = 3$  V and  $V_D = 1$  V), resulting from the very small channel and the reduction of grain boundaries and defects under the gate area.

#### ACKNOWLEDGMENT

The authors would like to thank MOE-ATU and NSC, Taiwan for financial support and National Nano Device Laboratories for facility utilization.

#### REFERENCES

- [1] S. M. Fluxman, "Design and performance of digital polysilicon thin-film-transistor circuits on glass," *IEEE Proc. Circuits Devices Syst.*, vol. 141, no. 1, pp. 56–59, Feb. 1994.
- [2] M. Rodder and S. Aur, "Utilization of plasma hydrogenation in stacked SRAM's with poly-Si PMOSFET's and bulk-Si NMOSFET's," *IEEE Electron Device Lett.*, vol. 12, no. 5, pp. 233–235, May 1991.
- [3] S. Zhang, R. Han, J. K. O. Sin, and M. Chan, "A novel self-aligned double-gate TFT technology," *IEEE Electron Device Lett.*, vol. 22, no. 11, pp. 530–532, Nov. 2001.
- [4] Y.-C. Wu, P.-W. Su, C.-W. Chang, and M.-F. Hung, "Novel twin poly-Si thin film transistors EEPROM with trigate nanowire structure," *IEEE Electron Device Lett.*, vol. 29, no. 11, pp. 1226–1228, Nov. 2008.
- [5] J.-T. Sheu, P.-C. Huang, T.-S. Sheu, C.-C. Chen, and L.-A. Chen, "Characteristics of gate-all-around twin poly-Si nanowire thin-film transistors," *IEEE Electron Device Lett.*, vol. 30, no. 2, pp. 139–141, Feb. 2009.
- [6] T.-F. Chen, C.-F. Yeh, and J.-C. Lou, "Effect of grain boundaries on performance and hot-carrier reliability of excimer-laser annealed polycrystalline silicon thin film transistors," *J. Appl. Phys.*, vol. 95, no. 10, pp. 5788–5794, May 2004.
- [7] M. K. Hatalis and D. W. Greve, "Large grain polycrystalline silicon by low-temperature annealing of low pressure chemical vapor deposited amorphous silicon films," *J. Appl. Phys.*, vol. 63, no. 7, pp. 2260–2266, Apr. 1988.
- [8] S.-W. Lee and S.-K. Joo, "Low temperature poly-Si film transistor fabrication by metal induce lateral crystallization," *IEEE Electron Device Lett.*, vol. 17, no. 4, pp. 160–162, Apr. 1996.
- [9] C.-W. Lin, L.-J. Cheng, Y.-L. Lu, Y.-S. Lee, and H.-C. Cheng, "High-performance low-temperature poly-Si TFTs crystallized by excimer laser irradiation with recessed-channel structure," *IEEE Electron Device Lett.*, vol. 22, no. 6, pp. 269–271, Jun. 2001.
- [10] H.-C. Cheng, F.-S. Wang, and C.-Y. Huang, "Effects of NH<sub>3</sub> plasma passivation on N-channel polycrystalline silicon thin-film transistors," *IEEE Electron Device Lett.*, vol. 44, no. 1, pp. 64–66, Jan. 1997.
- [11] H.-C. Lin, H.-H. Hsu, C.-J. Su, and T.-Y. Huang, "A novel multiple-gate polycrystalline silicon nanowire transistor featuring an inverse-T gate," *IEEE Electron Device Lett.*, vol. 29, no. 7, pp. 718–720, Jul. 2008.
- [12] C.-J. Su, T.-I. Tsai, Y.-L. Liou, Z.-M. Lin, H.-C. Lin, and T.-S. Chao, "Gate-all-around junctionless transistors with heavily doped polysilicon nanowire channels," *IEEE Electron Device Lett.*, vol. 32, no. 4, pp. 521–523, Apr. 2011.
- [13] T.-C. Liao, S.-W. Tu, M.-H. Yu, W.-K. Lin, C.-C. Liu, K.-J. Chang, Y.-H. Tai, and H.-C. Cheng, "Novel gate-all-around poly-Si TFTs with multiple nanowire channels," *IEEE Electron Device Lett.*, vol. 29, no. 8, pp. 889–891, Aug. 2008.
- [14] W.-C. Chen, C.-D. Lin, H.-C. Lin, and T.-Y. Huang, "A Novel double-gated nanowire TFT and investigation of its size dependency," in *Proc. Int. Symp. VLSI Technol. Syst. Appl.*, Apr. 2009, pp. 121–122.
- [15] M. Im, J.-W. Han, H. Lee, L.-E. Yu, S. Kim, C.-H. Kim, S. C. Jeon, K. H. Kim, G. S. Lee, J. S. Oh, Y. C. Park, H. M. Lee, and Y.-K. Choi, "Multiple-gate CMOS thin-film transistor with polysilicon nanowire," *IEEE Electron Device Lett.*, vol. 29, no. 1, pp. 102–105, Jan. 2008.
- [16] C.-M. Lee and B.-Y. Tsui, "High-performance poly-Si nanowire thin-film transistors using the HfO<sub>2</sub> gate dielectric," *IEEE Electron Device Lett.*, vol. 32, no. 3, pp. 327–329, Mar. 2011.